Integration of carbon nanotubes into diluted magnetic semiconductor

Yun-Hi Lee,[a] J. M. Yoo, J. Ah Lee, S. Y. Ahn, J. Joo, and S. Lee
Department of Physics and Center for Integrated Nano System, Korea University, Sungbuk-ku, Seoul 136-713, Korea

D. H. Kim
Department of Physics, Yeungnam University, Kyungsan, Korea

B. K. Ju
College of Engineering, Korea University, Seoul 136-701, Korea

K. J. Song
Applied Superconductivity Group, KERI, Changwon, Korea

(Received 11 April 2005; accepted 5 August 2005; published online 16 September 2005)

Carbon nanotubes (CNTs) were grown using catalytic pyrolysis of acetylene on a thin-film-diluted magnetic semiconductor (Co-8 at. % doped TiO_2) without consuming the host layer of semiconductor TiO_2. Effects of the thickness of the diluted magnetic semiconductor layer and the stacking structure on the growth of the carbon nanotubes were examined. The external diameter and crystalline structure of the nanotubes showed correlation with the structure of the magnetic catalyst Co within the nanotubes or at the end of the tube. After the growth of CNTs, the TiO_2 layer still maintained its semiconducting properties in view of the temperature dependent resistance behavior. Moreover, we studied the influence of the electrical resistivity, i.e, the thickness as a process parameter, of the diluted magnetic semiconductor underlayer, which determines the growth height and the crystalline quality of the carbon nanotubes, on the nanotubes' growth behavior. Finally, we measured the magnetic behavior of the heterosystem and interpreted the results due to the action of the properties of the catalytic diluted magnetic semiconductor underlayer. Our result shows a promising recipe for the fabrication of one-dimensional CNT—two-dimensional magnetic-metal-doped magnetic semiconductor and/or wide-band-gap insulator. © *2005 American Institute of Physics*. [DOI: 10.1063/1.2045557]

One-dimensional carbon nanotubes (CNTs) may provide the bridge connecting conventional micromaterials, microelectronics and nanoelectronics. They also serve as the electrodes, active channels of nanoelectronic elements, and key sensing elements in chemo-bio sensors.[1–7] Because all of the attempted approaches to nanoelectronics require major challenges in technology, they are most likely to become practical if they can be implemented onto the conventional silicon electronics and, furthermore, the CNTs should be integrated directly during the fabrication process onto pre-defined various electronic components.[8,9]

Explosive studies in the spintronics field have made it possible to fabricate various diluted magnetic semiconductor (DMS) materials.[10–15]

In this work, we report the possibility of creating a CNT-DMS junction using catalytic CVD methods. Especially, the main work is to realize the growth of CNTs with a Co-doped TiO_2-diluted magnetic semiconductor as a single matrix, including the catalyst (Co) and the supporting semiconductor material (TiO_2). Furthermore, considering that Ti-based materials are wettable with CNT, it could be expected that TiO_2-based substances provide good contact properties between CNT and DMS.

All the Co-doped TiO_2 films were deposited, using the conventional radio frequency (rf) magnetron sputtering technique, on the 500-nm-thick thermally grown SiO_2-coated Si substrates with a resistance of about 0.01 cm. A 3 in. Co-doped (8 wt %) TiO_2 ceramic target was used and more details for the deposition process were described elsewhere.[16] Some parts of the prepared specimens with patterned DMS films were used to check whether DMS acted as a catalyst or not.

Figure 1 shows the atomic force microscope (AFM) images and the histogram of the particle size distribution of the TiO_2:Co films just before the growth of the CNTs. As is known, in catalytic CVD growth, a secondary phase material, referred to as either a catalyst or an impurity, is purposely introduced to confine the crystal growth to a specific orientation and within a specific area. Normally, a catalyst forms a liquid droplet (i.e., a nanoparticle) by itself or by alloying with a growth material during the growth,[17,18] which acts as a trap of the growth species. The catalyst or impurity must be chemically inert and must not react with chemical species such as by-products presented in the growth reactor. A typical elemental compositional spectrum of the DMS film was examined with XPS (reported elsewhere). It is well known that although a small grain size is not guaranteed in an as-deposited DMS, further steps appear to assist the breakdown of the DMS films into the desired nanoparticles. In our method, a mixture of H_2 and NH_3 is used before admitting the feed gas (C_2H_2) and initiating growth. During this step, the thin film DMS is transformed into nanoparticles, maintaining adherence to the bulk of the DMS film, as illustrated in Figs. 1(a)–1(e). Although no completely forming nano islands were seen, roughening of the surface and then clustering were observed upon pre-treatment, as shown in Fig. 1(a). As expected, a thicker film, shown in Figs.

[a]Author to whom correspondence should be addressed; electronic mail: yh-lee@korea.ac.kr

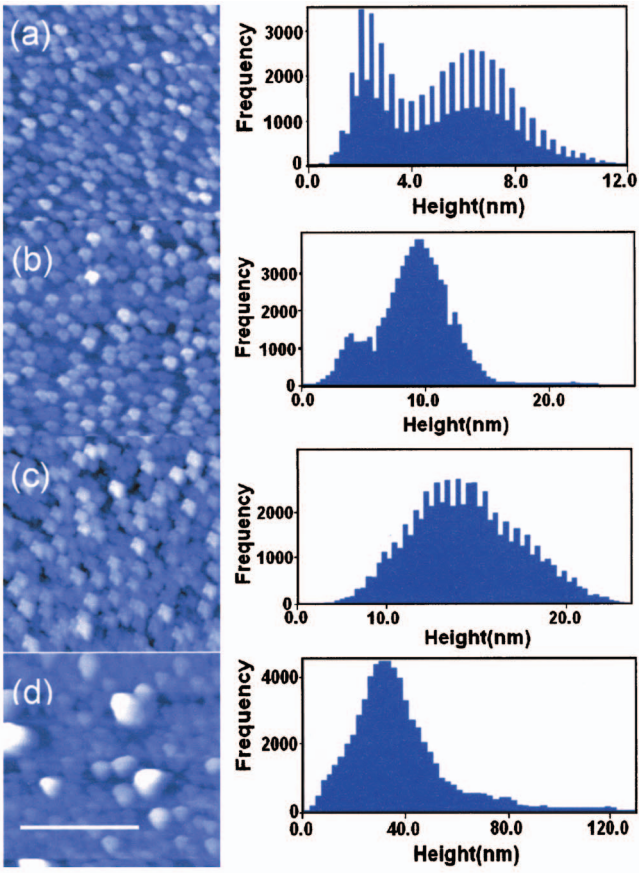

FIG. 1. (Color) Two-dimensional AFM images taken from the top of the DMS underlayer after pre-treatment. Each of the figures from (a)–(b) corresponds to 6-, 14-, 90-, and 180-nm-thick DMSs, respectively. The right-hand-side figure shows the histogram of the roughness distribution of the topmost of the DMS films.

1(b)–1(d), showed a bigger grain size. On the other hand, a further increase in the DMS thickness did not result in an increase of the grain size, and no further increase indicated that there is a maximum droplet size that is achievable by thin films, resulting from the reaction of TiO_2:Co with the Si substrate.

Figure 2(a) shows NTs formed on a patterned silicon substrate using the TiO_2:Co layer. Although the patterns in Fig. 2(a) appear to be neat and well aligned, high-resolution SEM images [Fig. 2(b)] reveal that the NTs grow like vines and support each other due to the van der Waals force, i.e., the crowding effect. The feedstock was acetylene heated at a substrate temperature of 800 °C for 10 min.

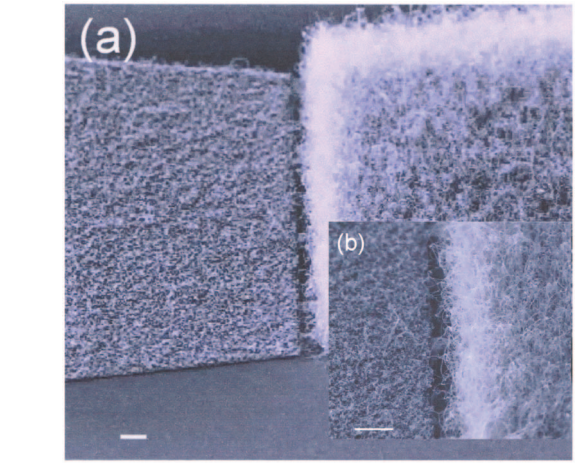

FIG. 2. (Color) (a) A typical SEM picture of a CNT grown on a substrate, showing the selective growth on the patterned DMS site. (b) A magnified image of the same specimen. We can easily observe the entangled CNTs with imperfect appearances, although, at first glance, that shown in (a) seems to be well aligned.

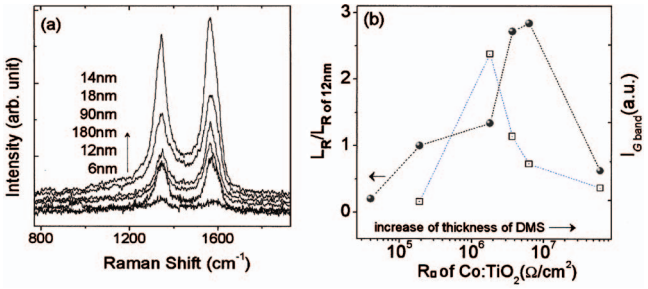

FIG. 3. (Color) (a) The Raman spectra of the tangential modes of several CNT specimens grown using DMS layers with different thicknesses. (b) The normalized growth height of the $L(t)/L$ (thickness of DMS=12 nm) of CNTs as a function of sheet resistance, obtained with different thicknesses of the DMS layer.

Raman spectra were examined as a function of the thickness of the DMS layer, as shown in Fig. 3(a). Varying the DMS thickness yielded best results in terms of structural quality through the Raman scattering characteristics with 14 nm of DMS. At a high frequency of above 1200 cm^{-1}, there were two tangential mode peaks for the CNTs grown onto the DMS layer, while the peak intensity and position varied with the thickness of the catalytic DMS layer. The strongest peaks of the CNTs were located at 1580 and 1350 cm^{-1}, respectively. The D/G ratio and sharper G band features[19] were maintained at a DMS thickness of up to 45 nm, beyond which the ratio and intensity of the peaks decreased drastically. For the DMS samples, the electrical resistivity of the TiO_2:Co with varying thicknesses, which was determined using the four-point method, was studied. Figure 3(b) shows the effects of the sheet resistance of the DMS on the growth height of CNTs and the intensity of the *G* band in the Raman mode. The systematic increase in the sheet resistance with the increasing thickness of the DMS was observed, and the relative increase in the growth height as well as the intensity of the *G* band was higher at about 14–90 nm. Beyond 90 nm, a rapid decrease occurred with

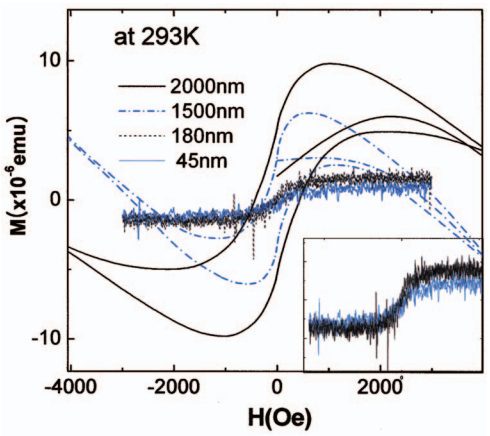

FIG. 4. (Color) (a) UV-VIS absorption spectra of TiO_2:Co and CNT onto TiO_2:Co. (b) Observed ferromagnetic hysteresis loop for the specimens at 293 K, obtained using PPMS and AGM measurements. Inset figure shows enlarged loops corresponding to the 180- and 45-nm-thick catalytic TiO_2:Co layer.

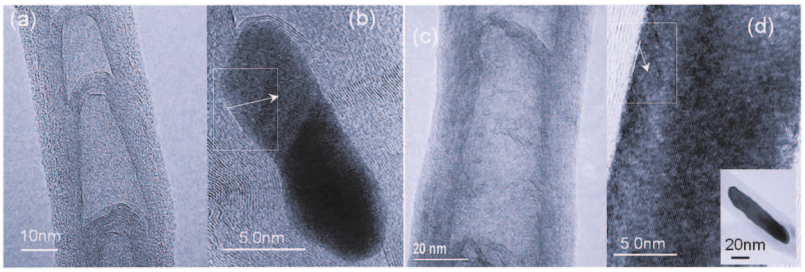

FIG. 5. (Color) (a) The SEM image of an individual CNT grown using a stoichiometric DMS. The image shows well-defined compartments. (b) A typical residue enclosed in the compartment of the CNT of (a). (c) The SEM image of an individual CNT grown using an oxygen-deficient DMS.

the increasing resistance of the DMS. For the as-deposited TiO_2:Co specimen, which is essentially a large-gap semiconductor, it was confirmed that the absolute value of the sheet resistance was very high, and with the increase in the thickness of the TiO_2:Co layer, a remarkable increase in the electrical resistance resulted in the range of a few hundred $\sim 10^8\ \Omega$ cm. From the assessed relationship between the thickness of the DMS and the structural purity (i.e., the intensity of the *G* band) of CNTs, it will be noted that CNTs are higher in samples with thicker layers of DMS. Within the thickness range in our test, such a trend was observed consistently.

Figure 4 shows the magnetization versus magnetic field taken at room temperature (RT) for the samples as a function of catalytic TiO_2:Co underlayer. Magnetization curves show a clear hysterestic behavior with a remanence approximately 60% of the saturation magnetization and Curie temperature (T_c) above room temperature for all samples tested in this study. The saturation magnetization value is 9.7×10^{-6} emu for the 5 mm $\times$ 5 mm dimension. Although magnetization measurements reveal little difference in hysteresis itself, transport measurements indicate otherwise (will be reported as a separate article).

Finally, to investigate the effect of the composition of the topmost of TiO_2:Co layer, which was assumed to act effectively during the growth of CNT in our catalytic RT CVD process, on the structural properties of residue within a individual CNTs, a HRTEM measurement was carried out for the two kinds of catalytic TiO_2:Co layers having different amounts of oxygen content. Figure 5(a) shows the HRTEM images taken of CNTs on a stoichiometric and oxygen-deficient TiO_2:Co, respectively. The individual CNT shows a peculiar bamboo-like shape within its body, showing a difference in the perfection of its structure. The DMS with a stoichiometric surface leads to the formation of perfect bamboo-like structures within the body of the CNTs. The tube consists of a linear chain of hollow compartments that are spaced at nearly equal distances (from 20 to 30 nm) from the stoichiometric and oxygen-deficient TiO_2:Co CNTs, respectively. The outermost surface of the stoichiometric CNT was covered by a thick, amorphous carbon layer, and a thinner layer was formed in the oxygen-deficient TiO_2:Co CNT. On the other hand, in the latter case, one end of the tube is capped with a DMS particle, which is in the normal Co phase, and the length of the residue is about a few tens of nm or longer, in contrast to the 10–15 nm length of the Co in the former CNTs. The enclosed residues in each compartment are in the form of nanoparticles, leaving inner sections of the CNTs free of DMS residues, and the DMS atoms enclosed in the CNTs have merged together to form large nanoparticles. Another distinct difference observed between these images is the direction of the crystallite phase, the lattice plane of which was perpendicular to the innermost wall in the former case and slanted to the innermost of the CNTs in the latter case.

In summary, we successfully demonstrated, for the first time, the possibility of an *in situ* junction of CNT and DMS via the catalytic rapid thermal CVD process.

This work was supported by the National R & D Project for Nano Basil Science and Technology (I) of MOST in Korea, and partially by the Korea Research Foundation (KRF-2004-005-D00087).

[1] S. J. Tans, A. R. M. Verschueren, and C. Dekker, Nature (London) **393**, 49 (1998).
[2] J. Kong, H. T. Soh, A. M. Cassell, C. F. Quate, and H. J. Dai, Nature (London) **393**, 878 (1998).
[3] A. Bachtold, C. Strunk, J. P. Salvetat, J. M. Bonard, L. Forró, T. Nussbaumer, and C. Schönenberger, Nature (London) **397**, 673 (1999).
[4] P. G. Collins, M. S. Arnold, and Ph. Avouris, Science **292**, 706 (2001).
[5] K. Besteman, J. O. Lee, F. G. M. Wiertz, H. A. Heering, and C. Dekker, Nano Lett. **3**, 727 (2003).
[6] Q. M. Hudspeth, K. P. Nagle, Y.-P. Zhao, T. Karabacak, C. V. Nguyen, M. Meyyappan, G.-C. Wang, and T.-M. Liu, Surf. Sci. **515**, 453 (2002).
[7] J. Nygard and D. H. Cobden, Appl. Phys. Lett. **79**, 4216 (2001).
[8] Y.-H. Lee, Y. T. Jang, D. H. Kim, J. H. Ahn, and B. K. Ju, Adv. Mater. (Weinheim, Ger.) **13**, 1371 (2001).
[9] H. Soh, C. Quate, A. Morpurgo, C. Marcus, J. Kong, and H. Dai, Appl. Phys. Lett. **75**, 627 (1999).
[10] Y. Matsumoto, M. Murakami, T. Shono, T. Hasegawa, T. Fukumura, M. Kawasaki, P. Ahmet, T. Chikyov, S. Koshihara, and H. Koinuma, Science **291**, 854 (2001).
[11] D. H. Kim, J. S. Yang, K. W. Lee, S. D. Bu, T. W. Noh, S.-J. Oh, Y.-W. Kim, J.-S. Chung, H. Tanaka, H. Y. Lee, and T. Kawai, Appl. Phys. Lett. **81**, 2421 (2002).
[12] S. A. Chambers, S. M. Heald, and T. Droubay, Phys. Rev. B **67**, 100401 (2003).
[13] S. R. Shinde, S. B. Ogale, J. S. Higgins, H. Zheng, A. J. Millis, V. N. Kulkarni, R. Ramesh, R. L. Greene, and T. Venkatesan, Phys. Rev. Lett. **92**, 166601 (2004).
[14] J. D. Bryan, S. M. Heald, S. A. Chambers, and D. R. Gamelin, J. Am. Chem. Soc. **126**, 11640 (2004).
[15] C. K. Yang, J. Zhao, and J. P. Lu, Phys. Rev. Lett. **90**, 257203 (2003).
[16] Y.-H. Lee, J. M. Yoo, D. H. Park, and B. K. Ju, Appl. Phys. Lett. **86**, 033110 (2005).
[17] N. M. Rodriguez, J. Mater. Res. **8**, 3233 (1993).
[18] H. T. Ng, B. Chen, J. E. Koehne, A. M. Cassell, J. Li, J. Han, and M. Meyyappan, J. Phys. Chem. B **107**, 8484 (2003).
[19] M. Souza, A. Jorio, C. Fantini, B. R. A. Neves, M. A. Pimenta, R. Saito, A. Ismach, E. Joselevich, V. W. Brar, G. G. Samsonidze, G. Dresselhaus, and M. S. Dresselhaus, Phys. Rev. B **58**, R16016 (1998).